

Dynamics of dendritic polymers in the bulk and under confinement

K. Chrissopoulou, S. Fotiadou, K. Androulaki, I. Tanis, K. Karatasos, D. Prevosto, M. Labardi, B. Frick, and S. H. Anastasiadis

Citation: [AIP Conference Proceedings](#) **1599**, 250 (2014); doi: 10.1063/1.4876825

View online: <http://dx.doi.org/10.1063/1.4876825>

View Table of Contents: <http://scitation.aip.org/content/aip/proceeding/aipcp/1599?ver=pdfcov>

Published by the [AIP Publishing](#)

Articles you may be interested in

[Analytical model for the dynamics of semiflexible dendritic polymers](#)

J. Chem. Phys. **136**, 154904 (2012); 10.1063/1.3703757

[Dendrite growth in annealed polymer blends for use in bulk heterojunction solar cells](#)

J. Appl. Phys. **110**, 103517 (2011); 10.1063/1.3652858

[Neutron scattering study of the dynamics of a polymer melt under nanoscopic confinement](#)

J. Chem. Phys. **131**, 174901 (2009); 10.1063/1.3258329

[Stretch dynamics of flexible dendritic polymers in solution](#)

J. Chem. Phys. **114**, 2430 (2001); 10.1063/1.1334660

[Dynamics of confined polymer chains](#)

J. Chem. Phys. **67**, 52 (1977); 10.1063/1.434540

Dynamics of Dendritic Polymers in the Bulk and Under Confinement

K. Chrissopoulou^a, S. Fotiadou^{a,b}, K. Androulaki^{a,c}, I. Tanis^b, K. Karatasos^b, D. Prevosto^d, M. Labardi^d, B. Frick^e and S. H. Anastasiadis^{a,c}

^a*Foundation for Research and Technology-Hellas, Institute of Electronic Structure and Laser, P.O. Box 1527, 711 10, Heraklion Crete, Greece*

^b*Aristotle University of Thessaloniki, Department of Chemical Engineering, Thessaloniki, Greece*

^c*University of Crete, Department of Chemistry, Heraklion Crete, Greece*

^d*CNR-IPCF, Department of Physics, University of Pisa, Pisa, ITALY*

^e*ILL-Institut Laue-Langevin, Grenoble, France*

Abstract. The structure and dynamics of a hyperbranched polyesteramide (Hybrane[®] S 1200) polymer and its nanocomposites with natural montmorillonite (Na⁺-MMT) are investigated by XRD, DSC, QENS, DS and Molecular Dynamics (MD) simulation. In bulk, the energy-resolved elastically scattered intensity from the polymer exhibits two relaxation steps, one attributed to sub- T_g motions and one observed at temperatures above the glass transition, T_g . The QENS spectra measured over the complete temperature range are consistent with the elastic measurements and can be correlated to the results emerging from the detailed description afforded by the atomistic simulations, which predict the existence of three relaxation processes. Moreover, dielectric spectroscopy shows the sub- T_g beta process as well as the segmental relaxation. For the nanocomposites, XRD reveals an intercalated structure for all hybrids with distinct interlayer distances due to polymer chains residing within the galleries of the Na⁺-MMT. The polymer chains confined within the galleries show similarities in the behavior with that of the polymer in the bulk for temperatures below the bulk polymer T_g , whereas they exhibit frozen dynamics under confinement at temperatures higher than that.

Keywords: Layered Silicates, Intercalation, Confinement, Polymer Dynamics.

PACS: 81.07.Pr, 81.05.Qk

INTRODUCTION

The dynamics of polymers in the bulk and, more recently, under confinement, is of great interest both because it greatly affects many of their macroscopic properties and because of the complexity it exhibits over many length- and time- scales [1,2]. Moreover, the equivalence in the behavior between polymer nanocomposites and thin polymer films has recently been quantitatively verified [3]. In this respect, intercalated polymer / layered silicate nanohybrids (PLSN) can offer a unique avenue to study the behavior of macromolecules in nanoscopic confinement by utilizing conventional analytical techniques on macroscopic specimens [4,5,6,7,8,9]. On the other hand, hyperbranched polymers (HBPs) have emerged during the recent years as a promising class of versatile materials for a broad range of novel nanoscale applications [10]. Their multiple functionality combined with their suitable nanosized dimensions and their cost-effective synthesis procedures, as compared to dendrimers, suffice to classify them as particularly suitable candidates in several high-added-value applications e.g., in nanolithography, as dispersion agents or surface modifiers, while they appear as promising candidates for cost-effective pharmaceutical (e.g., drug delivery) formulations. However, despite their great industrial importance, there are only few studies that address issues related to their detailed characterization and their structure-dynamics-properties relationships.

The current work refers to the investigation of the effect of polymer / clay interactions on the dynamics of a hyperbranched poly (ester amide), Hybrane. The dynamics was obtained in the bulk and under the severe confinement of ~0.5-1.0 nm when chains are intercalated between the layers of the inorganic material utilizing quasi elastic neutron scattering [11], broadband dielectric relaxation spectroscopy and molecular dynamics simulations.

EXPERIMENTAL PART

Hybrane S 1200, a hyperbranched polyesteramide [12] with a number-average molecular weight $M_n=1200$ g/mol, a radius of gyration, R_g , calculated utilizing MD simulations [13] to be 7.6-8.0Å and glass transition temperature of $T_g=315$ K was kindly supplied by DSM. Its nanocomposites with Na^+ -MMT (Southern Clay) were synthesized by solution mixing in water. The hybrids as well as the silicates were characterized by X-ray diffraction (XRD) in order to determine the interlayer spacing. Quasielastic high-resolution neutron backscattering experiments were performed at the IN10 spectrometer of ILL. Energy variation is performed by moving the monochromator and exploring the Doppler effect; the range of energy transfer is $-13 < \Delta E = \hbar\omega < 13 \mu\text{eV}$. The incident wavelength is $\lambda=0.6271$ nm, resulting in a range of accessible scattering vectors $0.5 \leq q \leq 2 \text{Å}^{-1}$. The experimental resolution function is obtained by measuring the silicate at 1.5K whereas the energy resolution is $0.49 \mu\text{eV}$. In addition to the measurements of the quasielastic spectra, the energy resolved elastic intensity scattered from the samples is studied as a function of temperature for $1.5 \leq T \leq 500$ K with a heating rate of 0.3K/min. Broadband dielectric spectroscopy was employed to investigate the dynamic response of Hybrane in the bulk, the pure clay and their nanohybrids. The Novocontrol Alpha high resolution dielectric analyzer was used to measure the impedance or complex dielectric function in a frequency range from 10 mHz to 10 MHz. The covered temperature range was between 140K and 420K. The sample holder, which constitutes of two parallel plate electrodes, was mounted in the special sample holder for dielectric measurements which is directly connected to the input terminals of the impedance analyzer. For the MD simulations, fully atomistic models comprised by 40 Hybrane molecules in the bulk state are generated through the use of the Amorphous Cell algorithm (Materials Studio, Accelrys Inc.). For the description of bonded and non-bonded interactions, energetic parameters according to the AMBER force-field have been utilized. For a direct comparison to QENS data, the intermediate incoherent dynamic function arising from the scattering of individual atoms was calculated directly in the inverse space.

RESULTS AND DISCUSSION

A series of Hybrane / Na^+ -MMT nanocomposites with polymer compositions that cover the complete composition range from pure polymer to pure clay has been synthesized utilizing solution intercalation in water followed by slow solvent evaporation and annealing. Figure 1 shows the X-ray diffraction patterns for the pure polymer (Fig. 1c), the inorganic material (Fig. 1b) and one of the nanocomposite with 30wt% polymer concentration (Fig. 1a). Na^+ -MMT shows a main (001) diffraction peak at $2\theta = 8.7^\circ \pm 0.1^\circ$ due to its layered structure, which corresponds to an interlayer distance of $d_{001} = 1.05 \pm 0.05$ nm, in agreement with the value given by the supplier. Hybrane is amorphous and its diffraction pattern exhibits only a weak amorphous halo. For Hybrane nanohybrid, the diffraction peak appears at $2\theta=4.3^\circ$ resulting in interlayer distance of $d_{001}=2.05$ nm, thus the nanocomposite show the intercalated structure. It is noted that this specific nanohybrid was selected to investigate the polymer dynamics under confinement since it is anticipated that at this composition, all polymer chains reside between the layers of the inorganic material and that there is no excess polymer outside the galleries.

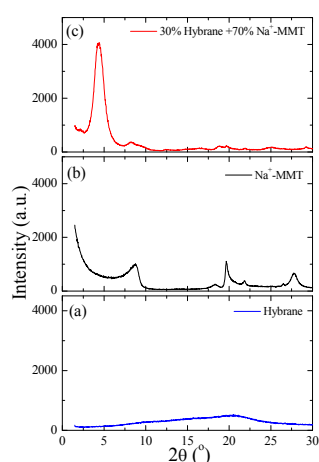


FIGURE 1: X-ray diffractograms of (a) Hybrane, (b) inorganic Na^+ -MMT and (c) a Hybrane: Na^+ -MMT 30:70 wt% nanohybrid

The dynamics of Hybrane in the bulk as well as under confinement was studied utilizing QENS and DS. Figure 2 shows the temperature dependence of the energy-resolved elastically scattered intensity of bulk Hybrane and the Hybrane nanocomposite at $q=1.45\text{\AA}^{-1}$. The curves are shown normalized at the lowest temperature $T=2\text{K}$ where all motions are frozen. The elastic intensity for the bulk polymer shows two distinct relaxation steps: the first step is a broad decrease at temperatures between ~ 80 and 220K . These temperatures are below the polymer glass transition and thus the main chain is still frozen, so the intensity drop should be attributed to local sub- T_g dynamic processes. The most common origin of such motions is due to the more mobile end- and/or side-groups, which, in this specific case, are the methyl and the hydroxyl groups attached to the polymer backbone. The second step in the elastic intensity for the bulk polymer is observed at temperatures higher than the calorimetric T_g and is caused by the motions of the polymer segments, which become unfrozen above the glass transition temperature. The elastic intensity of the nanocomposite with 30wt% Hybrane shows a step-like decrease similar to the respective of the bulk polymer for low temperatures that signifies the insensitivity of the very local motion to the confinement. Nevertheless, for temperatures higher than the Hybrane T_g , the elastic intensity does not drop to zero but shows a continuous decrease; this is very similar for all wavevectors. This means that after all sub- T_g motions have relaxed, there is no motion within the experimental window at these temperatures; i.e., the segmental dynamics is suppressed when the polymer is in the proximity of the inorganic surfaces within the galleries. QENS measurements of the incoherent structure factor have been performed at temperatures covering both the low- and high-temperature regimes, in order to study both the sub- T_g and the segmental motions for the bulk and the confined polymer.

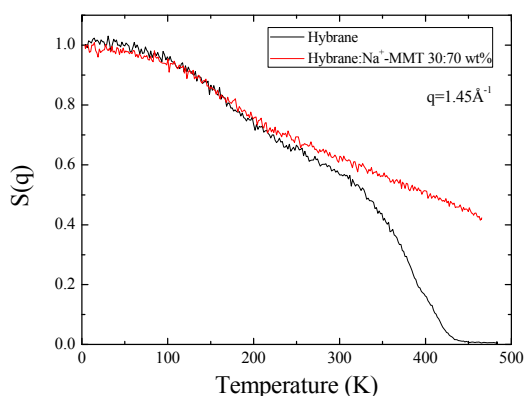


FIGURE 2: Energy resolved elastic scattered intensity for Hybrane and the 30wt% Hybrane nanocomposite

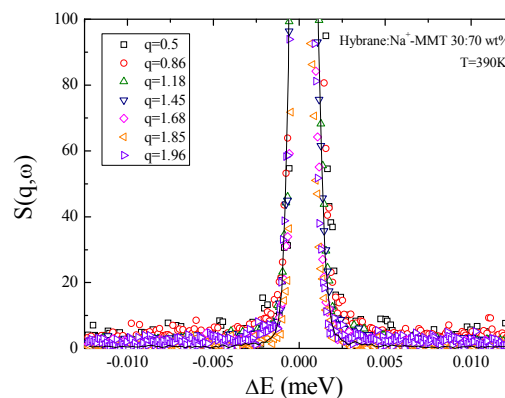


FIGURE 3: Incoherent structure factor, $S(q, \omega)$, of the nanocomposite with 30% Hybrane for various wavevectors at $T=390\text{K}$. The line is the instrumental resolution measured at temperature 2K . The y-axis is shown at 10% of the intensity of the data for the lowest q .

In conjunction with the elastic measurements, the quasielastic spectra measured at temperatures below T_g are very similar between the bulk Hybrane and the nanocomposite, resulting in very similar relaxation times (only slightly faster for the confined polymer) with a very weak (if any) wavevector and temperature dependence. Above the polymer T_g , the incoherent structure factor for the nanocomposites exhibits no broadening compared to the resolution function measured at $T=2\text{K}$, thus showing that all dynamics is completely frozen in the confined system in agreement with the elastic measurements (Figure 3). On the contrary, dynamics is present for the bulk polymer, but the pure segmental relaxation with the anticipated wavevector dependence of the relaxation time is recovered only at the highest temperature measured, i.e., at $T=390\text{K}$, whereas at lower temperatures a coupled motion of the segmental relaxation with a motion of the polymer branches (predicted by molecular dynamics simulation) is observed.

To investigate polymer dynamics in a much broader time range, dielectric relaxation spectroscopy was employed. Figures 4 and 5 show the complex dielectric permittivity for the bulk and the confined system at a temperature below and above the bulk polymer T_g , respectively. At $T=243\text{K}$ (below T_g) a very broad process is observed for the bulk polymer which is attributed to the local beta process due to the motion of small side groups. Nevertheless, the respective process for the nanohybrid is much narrower indicating that there is an effect of the confinement even for this very local process. Moreover, an additional slower relaxation process is observed for the nanohybrid at temperatures below T_g that is absent for the bulk Hybrane and the presence of which is reminiscent of a similar relaxation process observed in other confined systems [4,7,8]. At temperatures above T_g , Hybrane shows the anticipated segmental relaxation whereas there is no indication of any relaxation process for the confined system.

This result is in agreement with the findings of QENS which showed frozen dynamics in the nanohybrid at temperatures above the bulk polymer T_g .

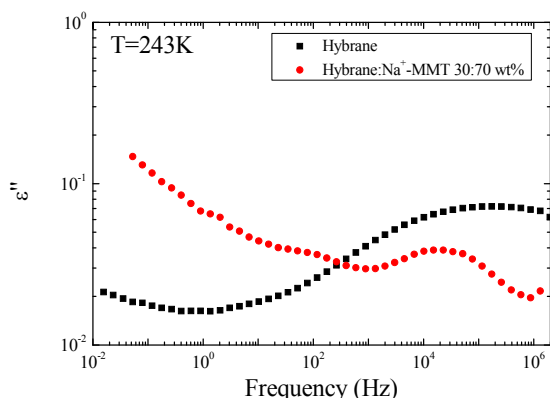


FIGURE 4: Frequency dependence of the dielectric loss ϵ'' for Hybrane and the nanocomposite at $T=243K$

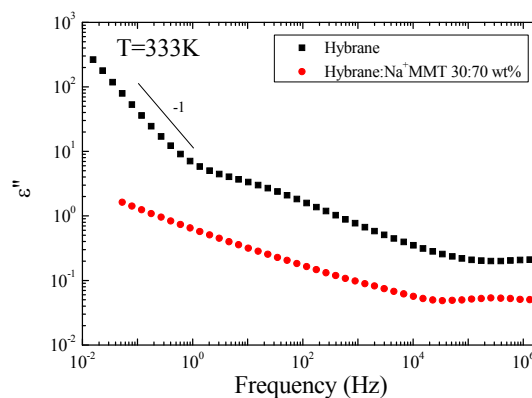


FIGURE 5: Frequency dependence of the dielectric loss ϵ'' for Hybrane and the nanocomposite at $T=333K$

ACKNOWLEDGMENTS

This research has been co-financed by the European Union (European Social Fund – ESF) and Greek national funds through the Operational Program "Education and Lifelong Learning" of the National Strategic Reference Framework (NSRF) - Research Funding Program: THALES - Investing in knowledge society through the European Social Fund (MIS 377278).

REFERENCES

1. J. Colmenero and A. Arbe, *J. Polym. Sci. Part B: Polym. Phys.* **51**, 87-113 (2013). V. G. Sakai and A. Arbe, *Curr. Opin. Colloid Interface Sci.* **14**, 381-390 (2009). H. N. Lee, K. Paeng, S. F. Swallen and M. D. Ediger *Science* **323**, 231-234 (2009).
2. S. K. Kumar and R. Krishnamoorti *Ann. Rev. Chem. Biomol. Eng.* **1**, 37-58 (2010). Special Issue on "Progress in Dynamics in Confinement", R. Zorn, L. van Eijck, M. M. Koza, B. Frick Eds. [*Eur. Phys. J.-Sp. Top.* **189**, 1-302 (2010)]. G. B. McKenna *Europ. Phys. J.-Sp. Top.* **189**, 285-302 (2010).
3. A. Bansal, H. Yang, C. Li, K. Cho, B. C. Benicewicz, S. K. Kumar and L. S. Schadler *Nature Mater.* **4**, 693-698 (2005).
4. S. H. Anastasiadis, K. Karatasos, G. Vlachos, E. Manias and E. P. Giannelis *Phys. Rev. Lett.* **84**, 915-918, (2000).
5. K. Chrissopoulou, I. Altintzi, S. H. Anastasiadis, E. P. Giannelis, M. Pitsikalis, N. Hadjichristidis and N. Theophilou *Polymer* **46**, 12440-12451 (2005). K. Chrissopoulou, I. Altintzi, I. Andrianaki, R. Shemesh, H. Retsos, E. P. Giannelis and S. H. Anastasiadis *J. Polym. Sci., Part B: Polym. Phys.* **46**, 2683-2695 (2008). K. Chrissopoulou and S. H. Anastasiadis *Europ. Polym. J.* **47**, 600-613, (2011).
6. K. Chrissopoulou, S. H. Anastasiadis, E. P. Giannelis and B. Frick *J. Chem. Phys.* **127**, 144910 (2007). S. H. Anastasiadis, K. Chrissopoulou and B. Frick *Mater. Sci. Eng. B* **152**, 33-39, 2008.
7. M. M. Elmahdy, K. Chrissopoulou, A. Afratis, G. Floudas and S. H. Anastasiadis, *Macromolecules* **39**, 5170-5173, (2006). K. Chrissopoulou, A. Afratis, S. H. Anastasiadis, M. M. Elmahdy, G. Floudas, B. Frick, *Eur. Phys. J.—Spec. Top.* **141**, 267-271, (2007).
8. S. Fotiadou, K. Chrissopoulou, B. Frick and S. H. Anastasiadis *J. Polym. Sci., Part B: Polym. Phys.* **48**, 1658–1667 (2010).
9. K. Chrissopoulou, K. S. Andrikopoulos, S. Fotiadou, S. Bollas, C. Karageorgaki, D. Christofilos, G. A. Voyiatzis and S. H. Anastasiadis *Macromolecules* **44**, 9710-9722 (2011).
10. D. Yan, C. Gao, H. Frey *Hyperbarnched Polymers : Synthesis, Properties and Applications*. Wiley Series on Polymer Engineering and Technology, 2011
11. S. Fotiadou, C. Karageorgaki, K. Chrissopoulou, K. Karatasos, I. Tanis, D. Tragoudaras, B. Frick and S. H. Anastasiadis, *Macromolecules* **46**, 2842-2855 (2013).
12. P. Froehling *J. Polym. Sci., Part A: Polym. Chem.* **42**, 3110-3115, (2004).
13. I. Tanis, D. Tragoudaras, K. Karatasos and S. H. Anastasiadis *J. Phys. Chem. B* **113**, 5356-5368 (2009).